

Cosmological Constraints for a Varying Dark Energy Model

ABDULLAH ALSAKKA¹

¹*Umeå University
Universitetstorget 4, 901 87
Umeå, Sweden*

ABSTRACT

This paper uses the Pantheon+ data set that consists of 1701 light curves of 1550 unique type Ia Supernova to find constraints on various cosmological models and compare them with a varying dark energy model proposed by Chevallier, Polarski and Linder in the early 2000s and analyze it deeper. The results show a tipping point from a decelerating universe to an accelerating one at a redshift of $z = 0.35$, and a second tipping point back to a decelerating universe in the future at $z = -0.19$. The flat Chevallier-Polarski-Linder (CPL) model leads to a matter dominated universe with $\Omega_m = 0.52 \pm 0.08$ while the relative dark energy density $\Omega_{de} = 0.48 \pm 0.08$. Finally, taking all these models and comparing them with the results that are found from Taylor expanding the distance relation shows that they are mostly consistent with a deceleration parameter around $q_0 = -0.28$.

Keywords: Astronomy — Varying Dark Energy — Distances

1. INTRODUCTION

For centuries humans have been looking at the heavens in search of answers to deep questions about life and the universe, about who we are and where we are in this vast and enormous dark space. The more we looked further the more questions we asked, the more we realized that we know so little about what is going around us. This paper might add one little piece to our very limited knowledge of the universe, but more importantly might lead to bigger questions that we must look for.

In this paper; I use the Pantheon+ supernova (SN) data [Scolnic et al. \(2022\)](#) to dig deeper into a model of varying dark energy, and comparing the solutions from the Einstein's equations with a pure kinematic approach, based on a Taylor expansion of the Friedmann-Lemaître-Robertson-Walker (FLRW) metric.

1.1. *Brief History of SN Cosmology*

Supernovae are very powerful events that occur and are occurring all over the universe. Their high luminosity makes them easier to detect, and even in some cases see with the naked eye. Such events have been detected throughout history, ever since mankind gazed into the skies. Around year 185 A.D. the first records of a powerful and bright object in the skies emerged from ancient Chinese scripts, which now is believed to be a supernova event (Later named SN185). At the time it was thought to be a "guest star" and was visible for 8 months [Wikipedia contributors \(2023a\)](#). After several other "guest star" observations, a notable

one was recorded independently by Chinese, Japanese and Islamic astronomers in year 1054. Later named as SN1054, this is believed to be the birth of the Crab Nebula - a remnant still visible to this day [Wikipedia contributors \(2023b\)](#). Supernova events challenged our understanding of the world back then, it was contradicting with our belief of unchanging heavens (notably the SN observations made by Tycho and Kepler); and to this day it still challenges our understanding of the universe.

With modern technologies, telescopes and more sophisticated photometry & spectroscopy techniques; this field of astronomy blew up in the early 20th century, like many other fields in physics. In 1968, astronomers identified a type of supernova that lacked hydrogen lines in their spectra, which distinguished them from Type II supernovae. That was the beginning of Type I supernovae, and it was shown that these events had a well defined Hubble diagram which could provide good measurements of the Hubble constant [Kowal \(1968\)](#). It was later split into two classes: Type Ia and Type Ib/c [Doggett & Branch \(1985\)](#); [Uomoto & Kirshner \(1985\)](#); [Wheeler & Levreault \(1985\)](#); [Wheeler & Harkness \(1990\)](#); [Porter & Filippenko \(1987\)](#). Type Ia SN had a peak brightness between 0.4 mag and 0.6 mag and they were initially believed to be the explosion of white dwarf stars accreting mass from a companion star until they reach a critical mass, triggering a runaway nuclear fusion reaction. However, the exact nature of the companion star and the triggering mechanism remained uncertain. With stellar evolution theory the understanding of su-

pernovae improved. In a binary system, as the white dwarf’s mass reaches the Chandrasekhar limit (about 1.4 times the mass of the Sun), a thermonuclear explosion ensues, leading to a supernova [Hoyle & Fowler \(1960\)](#); [Arnett \(1969\)](#); [Colgate & McKee \(1969\)](#).

Scientists later realized that merely increasing the sample size was not enough, improving systematic errors was the real matter and thus started the attempts of finding and eliminating errors. Reddening by intergalactic dust was a real issue and was falsely corrected based on the wrong assumption that all SNe Ia had the same intrinsic color [Branch & Tammann \(1992\)](#). With more low redshift SNe discovered, a deeper understanding of SNe type Ia was established and led to the finding of a correlation between the brightness change in filter B after 15 days ($\Delta m_{15}(B)$) and the luminosity of the SN; the slower the SN brightness declined the more luminous it was [Phillips \(1993\)](#).

A more refined database was required for further investigations and thus many surveys were established such as the Supernova Cosmology Project [Perlmutter et al. \(1997\)](#) and the High-z Supernova Search Team [Schmidt et al. \(1998\)](#), which were major parts in the discovery of an accelerating universe [Riess et al. \(1998\)](#); [Perlmutter et al. \(1999\)](#). This milestone in cosmology and physics was awarded the Nobel prize in 2011.

Nowadays SNe are discovered more frequently, with different surveys concentrating on different redshift ranges. Pantheon+ [Scolnic et al. \(2022\)](#) is a project to refine and standardize the many surveys and compile them under one big data base of many different supernovae. It is the biggest attempt of packaging data so far with 1701 different light curves for 1550 distinct Type Ia SNe.

With the help of the Pantheon+ database the SH0ES (Supernova H0 for the Equation of State) team was able to determine a Hubble constant (H_0) of 73.04 ± 1.01 km s⁻¹ Mpc⁻¹ using the distance ladder method that was originally utilized by Edwin Hubble himself [Riess et al. \(2022\)](#). This new result for H_0 is even further to the cosmic microwave background (CMB) result from the Planck mission of 67.4 ± 0.4 km s⁻¹ Mpc⁻¹ [Aghanim et al. \(2020\)](#) when compared to the past trusted results. The Hubble tension (The difference between the two results) is worse than ever, this is why many new models and researches are being made in order to resolve this tension and better our understanding of the expansion of the universe.

1.2. This Paper

In this paper I use the data from the Pantheon+ research to find the cosmological parameters for a time

dependent dark energy model proposed by [Chevallier & Polarski \(2001\)](#); [Linder \(2003\)](#). I use two different methods to do so - one by using the results from the Einstein equations (EE), and one by using a Taylor expansion for distance from the FLRW metric - and compare them.

In section 2 I explain the Pantheon+ data set and the procedures it went through. A summary of the cosmological models and statistical analysis methods used in this study is shown in section 3, where their results are discussed deeply in section 4. A conclusion is finally presented in section 5.

2. DATA

The pantheon+ sample includes 18 different surveys with data that ranges from redshifts of $z = 0.001$ to $z = 2.26$. 1550 unique SN, with some measured by different surveys at the same time (which gives better systematic error), results in 1701 different light curves [Scolnic et al. \(2022\)](#). These light curves get fitted using the SALT2 model explained in section 2.1, which later go through a correction procedure - that will be explained in this section - in order to obtain the final and polished result, which is used in this paper.

2.1. SALT2 Model

The SALT2 (Spectral Adaptive Lightcurve Template 2) model [Guy et al. \(2007\)](#) is a widely used empirical model for fitting and analyzing the light curves of SNe Ia. It utilizes the intrinsic brightness and color of SNe Ia. The SALT2 model assumes that the light curve of a Type Ia SN can be described as a combination of a spectral template and a color parameter. The spectral template captures the shape of the supernova’s spectral energy distribution (SED) as it evolves over time, while the color parameter accounts for the color variation of the supernova with respect to a reference spectrum.

The model is based on a training set of well-observed SNe Ia with known distances and light curves. To fit the light curve of a specific Type Ia supernova using the SALT2 model; a modified version of the Tripp relation [Tripp \(1998\)](#) is used with parameters including the stretch factor, color, and time of maximum brightness. This fitting process provides estimates of the supernova’s intrinsic luminosity and its cosmological distance. With modifications made by [Kessler & Scolnic \(2017\)](#) the distance modulus could be found with

$$\mu = m_B - \alpha x_1 - \beta c - M - \delta_{\mu-\text{bias}}. \quad (1)$$

m_B is the apparent magnitude in band B, x_1 is the stretch of the light curve, c is the color, M is the absolute magnitude and finally $\delta_{\mu-\text{bias}}$ is a correction term to

account for selection biases that is determined from simulations following Popovic et al. Popovic et al. (2021). $\delta_{\mu\text{-bias}}$ includes δ_{host} , a correction term that relates the SN brightness with the host galaxy mass. All of these are explained in more detail in Brout et al. and Scolnic et al. Brout et al. (2022a); Scolnic et al. (2022).

m_B, x_1 and c can be found from light curve data while the rest are found by fitting equation (1) to the training set.

2.2. Selection Process

There are so many different events captured by the surveys, and figuring out which ones are SN events isn't an easy task. The light curves must pass through a selection process in order to be scientifically classified as a Type Ia supernova. First requirement is for the observation to be made before 5 days after the peak brightness, with a precision requirement for the peak brightness date up to 2 days; any observation made outside that period or with a bad precision is not taken into consideration. The light curves are trained over a set of SNe that are required to have $-3 < x_1 < 3$ and $-0.3 < c < 0.3$; furthermore, the error in x_1 has to be < 1.5 . Some observations of high redshift events are removed due to concerns about their systematic error Brout et al. (2022b).

After these selections and cuts, with some more that are mentioned more deeply in Scolnic et al., 1701 light curves remain from 1550 events classified as SN Ia.

2.3. Redshift Corrections

The light curves for both the model training process and the data fitting process have to account for some errors. In a cosmological sense, redshift is caused due to the expansion of the universe. However, one must not forget that both the Earth and the target objects might be in motion with respect to each other. The peculiar velocity corrected cosmic microwave background (CMB) is used to correct the redshift due to the motion of the SN in its host galaxy. The heliocentric correction for redshift takes into account the motion of Earth around the Sun, it basically takes the Sun as the reference point of the redshift measurement. These redshift corrections for the Pantheon+ data were provided by Carr et al. Carr et al. (2022).

2.4. Peculiar Velocities

Peculiar motion of galaxies can be due many reasons such as their flow in their cluster or supercluster. Peculiar velocities are used to correct the redshift data based on peculiar velocity maps drawn by large surveys. The peculiar velocities for the Pantheon+ data was deter-

mined by Peterson et al. who used multiple peculiar velocity maps and group catalogs Peterson et al. (2022).

2.5. Host Galaxy Properties

Effects such as dust in the host galaxy can cause errors in the light curves therefore corrections are made in two ways: simulations of the data that includes the correlations between color and stretch and host properties Popovic et al. (2021), and using (1) where $\delta_{\mu\text{-bias}}$ includes the host galaxy corrections.

2.6. Milky Way Dust Extinction

For low redshifts; one of the most prominent errors is the interstellar dust in our Milky Way which scatters and absorbs light, leading to a decrease in the observed brightness of astronomical objects. This extinction affects the observed colors and magnitudes of the SNe, causing a reddening effect. Therefore values of the extinction between the blue (B) and visual (V) bands, $E(B - V)_{\text{MW}}$, are applied to the SALT2 model fits.

3. COSMOLOGICAL THEORY

Even though supernovae of type Ia are used as distance indicators, they have to go through a calibration process with a training set that we know the distance of (using Cepheid variables or different methods) in order to determine the distances to the rest. Furthermore, their intrinsic magnitudes are not exactly the same but could vary. Different methods had to be utilized, most commonly using measurements of flux from the SN. The luminosity distance is defined as

$$d_L = \sqrt{\frac{L}{4\pi F}} \quad (2)$$

with L as the luminosity of the event and F being the flux measured at the telescope Hogg (1999). Luminosity is not easy to predict, but by using the Phillips' relation Phillips (1993) it can be empirically calculated. Scientists prefer to use the distance modulus as their distance indicator, however one must keep in mind that it is a relative distance and not a real physical distance.

With the use of FLRW metric one can relate the flux received at Earth with the luminosity of the star thus turning equation (2) into

$$d_L = \frac{c(1+z)}{H_0\sqrt{|\Omega_k|}} \mathcal{S} \left(\sqrt{|\Omega_k|} \int_0^z \frac{dz'}{E(z')} \right), \quad (3)$$

with

$$\mathcal{S}(x) = \begin{cases} \sinh x & \text{for open universe } \Omega_k > 0 \\ x & \text{for flat universe } \Omega_k = 0 \\ \sin x & \text{for closed universe } \Omega_k < 0 \end{cases} .$$

c is the speed of light, H_0 is the Hubble constant's present value and Ω_k is the curvature density component of the universe. Ω_k is not a real physical property and is just a mathematical expression given by $\Omega_k = -kc^2/H_0^2$ with k being the curvature constant in the FLRW metric (see appendix A for more insight). The function $E(z)$ describes how the Hubble parameter changes with redshift as $H(z) = H_0 E(z)$. In our case of varying dark energy, and a universe made of matter and dark energy $E(z)$ take the form of

$$E(z) = \sqrt{\Omega_m(1+z)^3 + \Omega_k(1+z)^2 + \Omega_{\text{de}} e^{(3 \int_0^z \frac{1+w(z')}{1+z'} dz')}} \quad (4)$$

$w(z)$ is the equation of state (EoS) for the dark energy component. The EoS is a parameter that describes the relation between pressure p and density ρ and gives us insights into the behavior and properties of cosmic components, it is defined by $p_i = w_i \rho_i$. This model includes the possibility of a constant EoS if $w(z) = w_0$. The density parameters Ω_m, Ω_k and Ω_{de} in equation (4) for matter, curvature and dark energy respectively describe their values at present time with their sum always being one ($\Omega_m + \Omega_k + \Omega_{\text{de}} = 1$). Using $E(z)$ we could also find the lookback time; which is the time light takes to travel from the source to us; or in other words how far in the past we are looking when observing an object in the sky. It can be found by

$$t_L = \frac{1}{H_0} \int_0^z \frac{dz'}{E(z')(1+z')} \quad (5)$$

Equation (4) comes from solving the Einstein equations (As shown in Appendix A). In order to solve equation (3) we can either use the result from Einstein equations (which assumes that the FLRW metric holds and that the EE are correct), or we can expand $H(z)$ to get a result that doesn't require the Einstein equations; that is

$$d_L = \frac{cz}{H_0} \left[1 + \frac{1}{2}(1 - q_0)z + \frac{1}{6}(3q_0^2 + q_0 + \Omega_k - j_0 - 1)z^2 \right] + \mathcal{O}(z^4). \quad (6)$$

The Hubble parameter $H = \dot{a}/a$, the deceleration parameter $q = -\ddot{a}a/\dot{a}^2$ and the jerk parameter $j = \ddot{\ddot{a}}a^2/\dot{a}^3$ with 0 as a subscript indicating the values at present time while Ω_k , the curvature density parameter, could only take values smaller than +1. Check Visser (2004) for proof of equation (6). This equation is a powerful one, because it is valid for all models and universes

that have a FLRW geometry, however one must keep in mind that this is an approximation and we can use it to whatever precision we desire by choosing the redshift limit from the data set. Equation (1) gives an empirical results, the theoretical definition of the distance modulus is

$$\mu = 5 \log d_L (\text{Mpc}) + 25. \quad (7)$$

To relate the empirical and the theoretical values of the distance modulus, a non linear curve fit that minimizes chi-squared (χ^2) is done, with χ^2 being

$$\chi^2 = \Delta \mathbf{D}^T \mathbf{C}^{-1} \Delta \mathbf{D}. \quad (8)$$

$\Delta \mathbf{D}$ is the residual vector and is given by

$$\Delta D_i = \mu_{\text{data},i} - \mu_{\text{model},i}$$

while \mathbf{C} is the covariance matrix given by the the Pantheon+ team. The covariance matrix includes systematic and statistical errors in the distance moduli (Check section 2.2 in Brout et al. (2022a)).

After fitting the curve and finding the parameters, one can relate the results from Einstein's equation with the results from the Taylor approximation using the deceleration parameter. The deceleration parameter's present value can be found from Einstein's equations using

$$q_0 = \frac{1}{2} \sum_i \Omega_i [1 + 3w_i(0)], \quad (9)$$

with the index Ω_i indicating the component's present density parameter value (This summation does not include Ω_k because as mention before it is not a real component with a physical meaning). For proofs of these equations check appendix A.

4. RESULTS AND DISCUSSION

Fitting various models by minimizing equation (8) would yield the best fit parameters for the different models in the Einstein equations result and for the Taylor expansion result. However; for the Einstein equations result, due to the amount of parameters in some model, the standard deviation will be high and therefore and therefore we will study special cases which are:

- Λ CDM model: $w(z) = -1$
- Flat w CDM model: $\Omega_k = 0, w(z) = w$
- Flat Chevallier-Polarski-Linder (CPL) Universe: $\Omega_k = 0, w(z) = w_0 + w_1 z/(1+z)$

The results are shown in Table 1 with the best fit plots in figure 1. For the Taylor series expansion it is quite

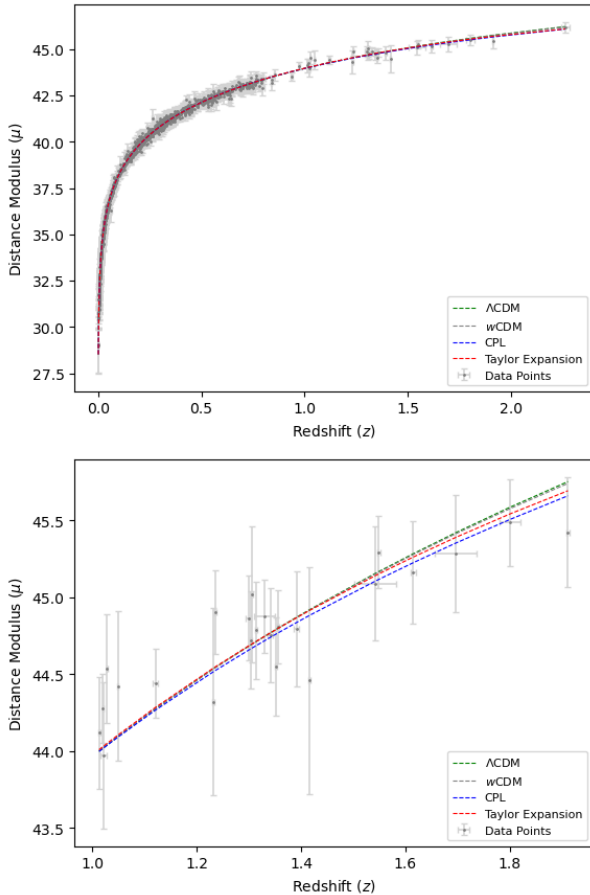


Figure 1. The Hubble diagram for the whole data set with all the models. The bottom graph is the Hubble diagram for $1 < z$ to better see the little deviations between the different models.

tricky to choose a set of redshifts to fit into, because the further you go the less accurate the approximation will be. However, the smaller the sample is the higher the standard deviations will be. For this study I decided to take the whole Pantheon+ sample, because - as it can be seen from figure 2 - the R^2 test is the highest with $R^2 = 0.952$ and the standard deviations are the lowest with the whole data set included.

4.1. Taylor Expansion

From figure 3 one can see how strongly a flat universe is supported with it being dead center in the confidence region, with a mean value of $2.2 \times 10^{-7} \pm 0.09$. That is inline with the base assumption of the FLRW metric, isotropy and homogeneity, which is also supported by the CMB observations of isotropy Aghanim et al. (2020). When looking at the deceleration one could see that the universe is in fact accelerating as first shown by the nobel prize winners of 2011 Riess et al. (1998); Perlmutter et al. (1999); Schmidt et al. (1998). The ef-

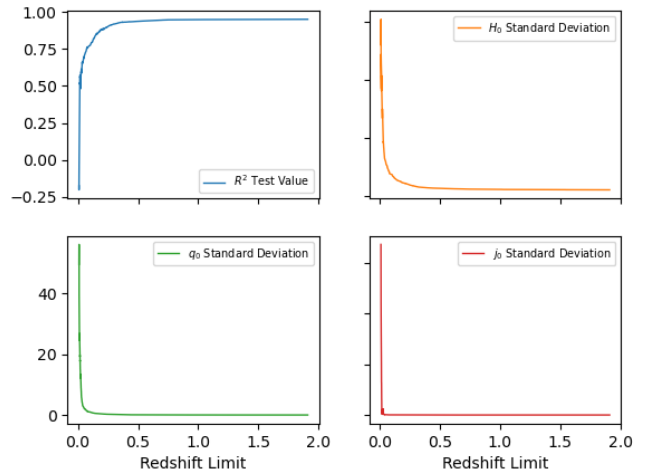


Figure 2. Graphs of the R^2 test values and standard deviations of the parameters against the redshift limit. One can see that R^2 reaches the maximum while the standard deviations reach the minimum with the whole data set

fects of curvature are valid from the 3rd degree term and above, but for our range of redshifts a 3rd degree estimate is enough because when we go up another degree we will have to introduce a new parameter which will lower our accuracy.

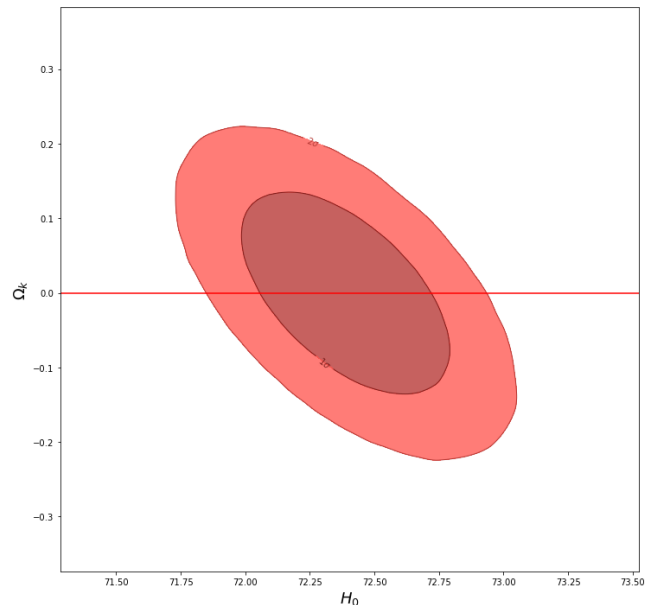


Figure 3. Contour map of confidence regions between the parameters q_0 and j_0 . The line shows $j_0 = 0$.

4.2. Λ CDM Model

For the Λ CDM model, quite interesting results can be seen. In the Pantheon+ analysis, the distance ladder method used in SH0ES was combined with the Hub-

Table 1. Parameters for different models, found by fitting the Hubble diagram using SN distances.

	H_0	Ω_m	Ω_{de}	Ω_k	w_0	w_1	q_0	j_0
Flat CPL Universe	72.17 ± 0.37	0.52 ± 0.08	0.48 ± 0.08	0	-0.92 ± 0.08	-1.55 ± 1.07	-0.17 ± 0.12	...
Λ CDM Universe	72.55 ± 0.28	0.26 ± 0.06	0.49 ± 0.08	0.25 ± 0.10	-1	0	-0.36 ± 0.09	...
Flat w CDM Universe	72.51 ± 0.28	0.21 ± 0.10	0.79 ± 0.10	0	-0.71 ± 0.13	0	-0.33 ± 0.19	...
Taylor Expansion	72.39 ± 0.26	$2.20e-07 \pm 0.09$	-0.28 ± 0.05	-0.26 ± 0.09

ble diagram fit yielding a result of $H_0 = 73.6 \pm 1.1$, $\Omega_m = 0.306 \pm 0.057$ and $\Omega_\Lambda = 0.666 \pm 0.018$ (which we indicate as Ω_{de} in this paper) for the Λ CDM model; which favored a flat universe Brout et al. (2022a). However in this analysis all free parameters were derived by solely analyzing SNe Ia (without the Cepheid variables in SH0ES). This yielded a smaller error in H_0 but larger errors in the density parameters, especially in Ω_Λ , as can be seen from table 1. Using the distance ladder method requires additional errors in the covariance matrix that correlates the Cepheids with the SNe Ia, therefore the error in the SH0ES analysis is larger for the Hubble constant. But on the other hand, constraining H_0 in the fit gives more accurate results for the density parameters. So the accuracy you lose in H_0 is transferred to the density parameters, and specifically Ω_Λ . The H_0 and Ω_m results in both analysis coincide within error ranges, however the results for Ω_Λ are very different favoring a more curved and open universe in this analysis compared to the Pantheon+ analysis. Even though this analysis of the Λ CDM model favors an open universe, a flat universe case can be found at around the 1.5σ boundary which means that an open universe can be found with 86.6% probability while the other 13.36% might be a flat or a closed universe, as shown in figure 4.

4.3. w CDM Model

The Λ CDM model is a case of the cosmological constant being the missing component in the universe that is causing an acceleration, aka dark energy. The w CDM model is a model which assumes that the missing component has a constant EoS value of w . Using the assumption of a flat universe, which is highly favored by the isotropy in the CMB measurements Aghanim et al. (2020), the results found are still contradictory with the Pantheon+ analysis of combining SH0ES; which gave $\Omega_m = 0.309^{+0.063}_{-0.069}$, $\Omega_\Lambda = 0.691^{+0.069}_{-0.063}$, $H_0 = 73.5 \pm 1.1$ and $w = -0.90 \pm 0.14$. This again is due to the same reasons mentioned in the Λ CDM case study. It can be seen clearly from figure 5 how using solely SNe Ia does not favor the cosmological constant being the dark energy component, but only when combined with Cepheid variables as done by the Pantheon+ team then there is a high possibility for a cosmological constant component causing the acceleration of the universe.

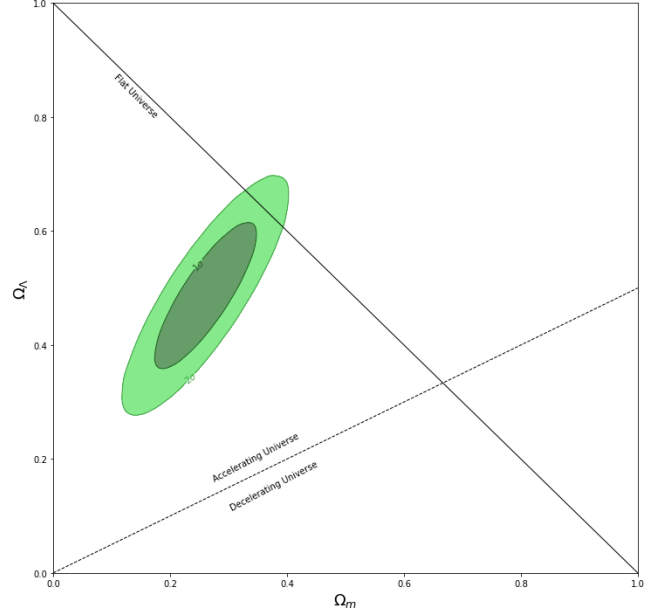


Figure 4. Contour map of confidence regions between the parameters Ω_m and Ω_Λ in the Λ CDM model. The solid line shows the values of $\Omega_m + \Omega_\Lambda = 1$ which results in a flat universe, while the dashed line shows $\Omega_m/2 - \Omega_\Lambda = 0$ which is the tipping point between an accelerating universe and a decelerating universe.

4.4. Chevallier-Polarski-Linder (CPL) Model

For our varying EoS case, I use the model suggested by Chevallier, Polarski and Linder Chevallier & Polarski (2001); Linder (2003)

$$w(z) = w_0 + w_1 \frac{z}{1+z}. \quad (10)$$

This model is just a simple mathematical expression of how the EoS might evolve, there is no specific physical meaning underlying this equation. Other varying EoS models are also proposed but they all share the same property that $\lim_{z \rightarrow 0} w = w_0$. With this model an analytical solution can be found for the exponential term in equation (4) yielding a dark energy component that changes with time as

$$\Omega_{de}(z) = \Omega_{de}(1+z)^{3(w_0+w_1+1)} e^{-3w_1 z/(1+z)}. \quad (11)$$

The results from this model gives a case of a matter dominated universe with 52% matter while the rest in

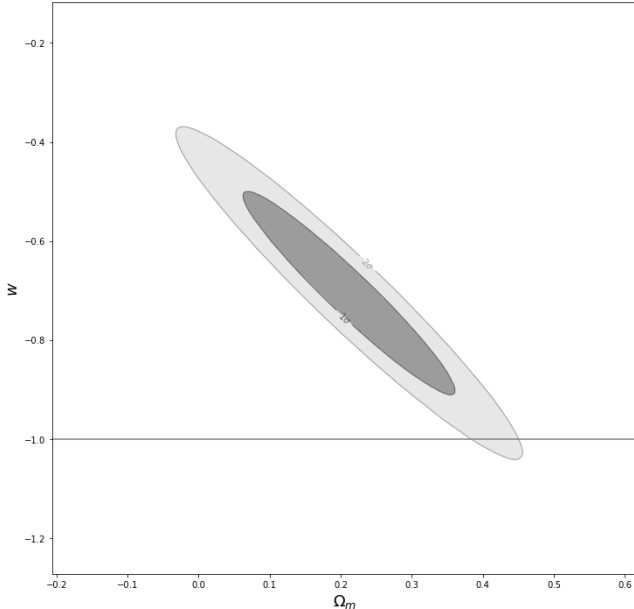


Figure 5. Contour map of confidence regions between the parameters Ω_m and w in the w CDM model. The solid line shows the value $w = -1$ which favors the cosmological constant as the dark energy component.

dark energy. This means that for an accelerating universe, a dark energy dominated case is not required and it could be achieved for a matter dominated universe by assuming varying EoS models. This is quite phenomenal, because a matter dominated universe means a decelerating universe! Is that the case? The Λ CDM model assumes constant dark energy while the w CDM assumes a dark energy that has a maximum at $z = \infty$, or the big bang. However for the CPL model, we have a defined extremum point for dark energy which can also be seen from figure 6 when plotting the dark energy as a function of redshift according to equation (11). This maximum point is found at $z = 0.052$, or around 700 million years ago. The CPL model also shows that the dark energy component seems to vanish in the future.

From figure 7 one can see that the deceleration starts positive and very high towards the beginning of the universe (high redshifts) and gets lower, which is an expected result since the matter density of the universe was very high (as it falls by $(1+z)^3$) and caused gravity to dominate and slow the expansion. Up till a tipping point where the expansion started to accelerate! This tipping point is predicted by the CPL model to be at $z = 0.35$ or 3.7 billion years ago. It keeps accelerating even faster after that point, but what differs this model from the others is that this acceleration reaches the maximum of $q = -0.19$ at $z = 0.08$, 1 billion years ago, and turns around after that reaching its value to

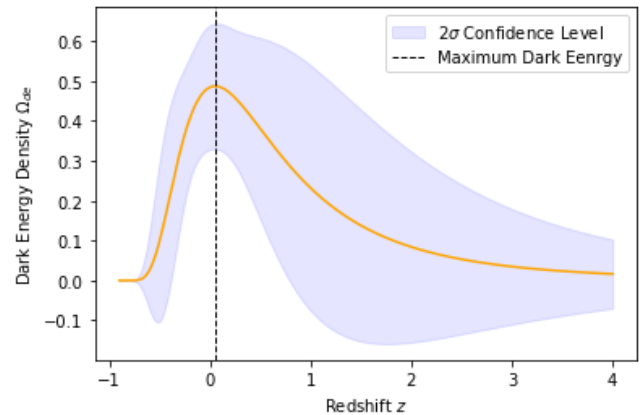


Figure 6. Dark energy density in the universe as a function of redshift, according to a flat CPL model. It is also extended to negative redshifts showing the future of the universe, by assuming it will always stay expanding. The dashed line shows where the dark energy density reaches its maximum value at $z = 0.052$.

day. It doesn't stop there! The acceleration keeps getting weaker until $z = -0.19$, 3.3 billion years in the future assuming that the expansion will continue, where it tips again and the universe starts to decelerate; reaching a maximum deceleration of $q = 0.20$ at $z = -0.431$. After that it looks like it stables at a constant expansion, however it is important to mention that for $z < -1$ we get into the mysterious realm of complex numbers. The positive values of the deceleration in the future are within 2σ confidence levels for some redshifts.

When checking the total density in figure 8, which can be interpreted as energy, we can see that this model follows a basic decreasing energy curve. This is what one might predict from any model, and it is relieving to see that the CPL model also follows the same trend. Even though the dark energy parameter turns around after a point and starts decreasing, the energy trend never increases and is consistently decreasing with time (from right to left). At the present, $z = 0$, the total energy density is 1; which is reconfirming our prior of flat universe.

The CPL model is supposed to be a more general case of most cosmological models, by not constraining the EoS to one value. It can be seen from figure 9 that the Λ CDM model falls within 1σ of the CPL confidence regions, while the w CDM model slightly coincides within error bars with the 2σ region.

Unfortunately, this model struggles to predict the age of the universe; with a result of $12.86^{+1.17}_{-0.93}$ billion years (found by evaluating at $z = \infty$ in equation (5)). The earliest and most distant object ever observed, GLASS-z12 observed by JWST in 2022 Naidu et al. (2022), falls on the far positive side of the error range. Compared

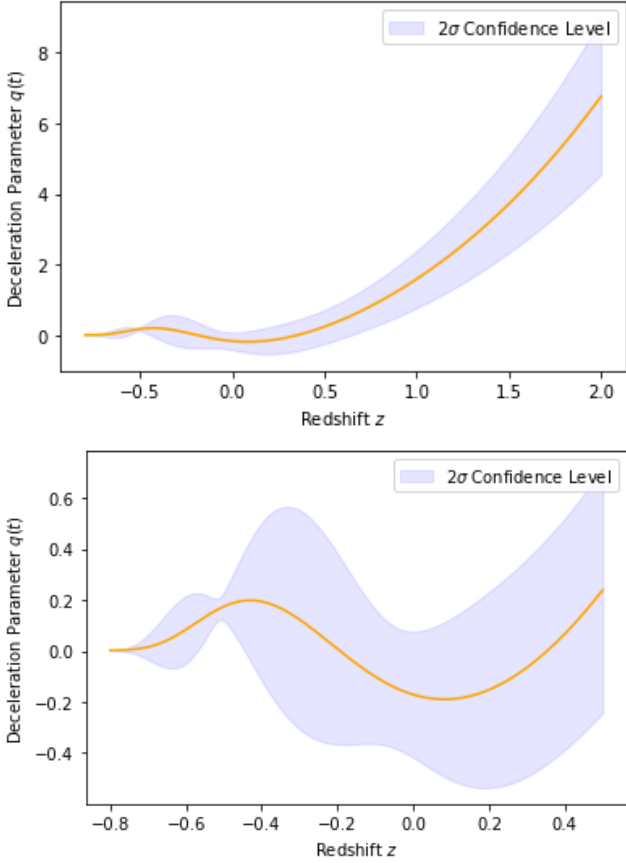


Figure 7. The deceleration parameter as a function of redshift for the CPL model. The plot is extended to negative redshifts to predict the future.

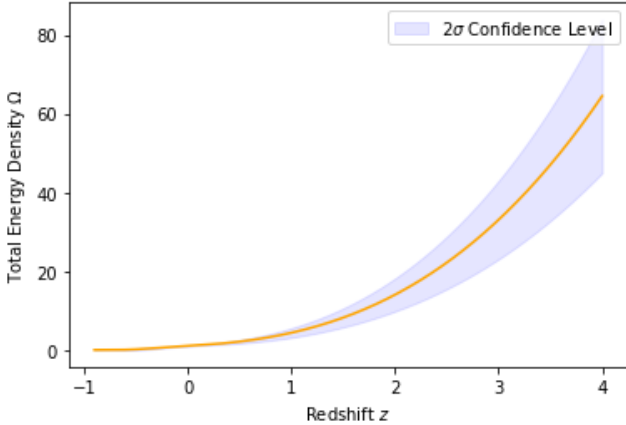


Figure 8. Total density (energy) in the CPL model can be seen to decrease from right to left, which is from the big bang until present time and into the future.

to the Λ CDM's $13.83^{+1.06}_{-0.83}$ billion years old universe and the w CDM's $13.83^{+2.34}_{-0.38}$ billion years old universe, the CPL model's age of universe is much smaller.

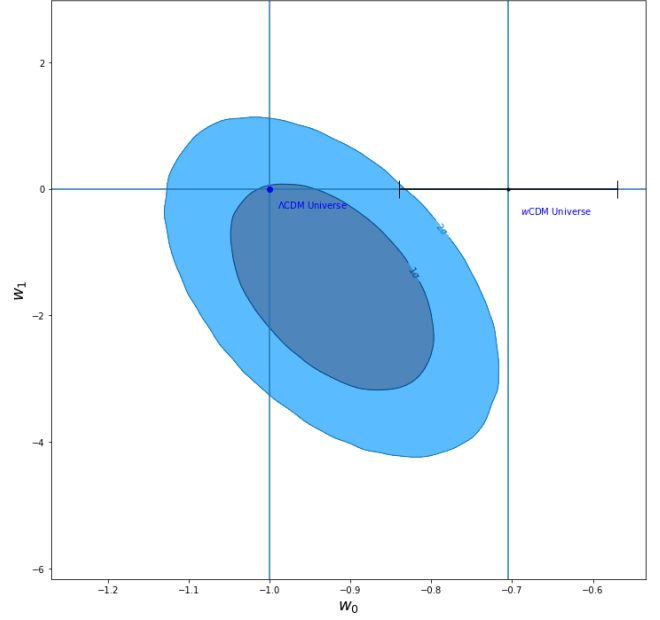


Figure 9. Contour map of confidence regions between the parameters w_0 and w_1 in the CPL model. The solid lines show the values at $w_0 = -1$ and -0.7 which are the Λ CDM and w CDM universes respectively. The errorbar in the w CDM's w is also shown.

4.5. Overview

These three models from the Einstein equations are not very distant in a sense. The Chavellier-Polarski-Linder model is the most general case of an additional unknown component in the universe that has an equation of state that may vary or may not, then the w CDM model holds this equation of state constant, while finally the Λ CDM model proposes that this unknown component is the cosmological constant from Einstein's equations - having an equation of state equal to -1 - and representing the vacuum energy in the universe since vacuum has a constant energy level that comes from quantum fluctuations. However when one measures the quantum fluctuations and compare it with the cosmological constant energy, the difference is in huge orders of magnitude [Carroll \(2001\)](#). Each of these models have their weak points and the points were they exceed, and while there is no way to determine which model is the absolute right one we can analyze them statistically and see which model explains the observations better. From figure 1 one can see that all four models follow the Hubble diagram consistently and that there are not big differences in the fits. When one looks at figure 10, then important conclusions can be drawn from the probability space of H_0 and Ω_m for the three Einstein equation models. While the Λ CDM model coincides almost perfectly with the w CDM model, being a more confined

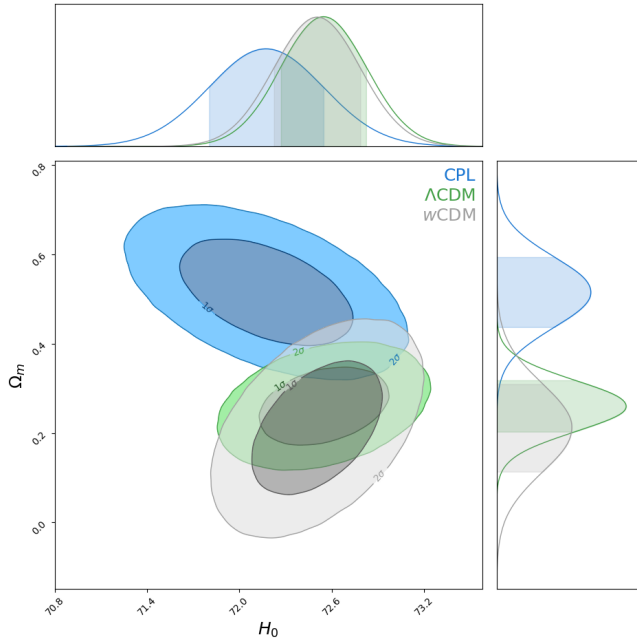


Figure 10. (H_0, Ω_m) probability space with all Einsteinian models studied in this paper.

region; the CPL model is in a higher matter density value with bigger regions due to higher standard deviations, but yet it is still very accurate ranging over small deviations. The CPL model does not coincide at all in a 1σ region with any of the two others, It is quite hard for a CPL universe to have the same combination of (H_0, Ω_m) with any of the other two.

From a Hubble constant point of view it can be seen that all these models have similar results which are quite far from the CMB results. The famous Hubble tension problem is yet to be understood, and even though the CPL model gets the nearest result to the CMB Hubble constant it still does not help with the Hubble tension problem. However one can argue that the changing EoS could have caused different properties of the universe in different times, perhaps that is why the two methods give different results. Maybe at $z = 1100$, where most of the CMB data comes from, the properties of dark energy were not the same and thus our understanding of the data is wrong [Valentino et al. \(2021\)](#).

For the Taylor expansion result; the deceleration parameter can't give us density parameters unless we assume a specific model, but for the Einsteinian models the density parameters can give us a deceleration parameter value. While most of them seem close, the CPL universe is much closer to zero. However when plotting the deceleration parameters' probability density functions we can see that they all coincide within 1σ in a specific region which is shown in figure 11 as the gray

shaded region. This region seems to be centered with the Taylor expansion's deceleration parameter, which is the only value that is not model dependent and mathematically reliable. Therefore we can say that all models are in agreement with the Taylor expansion's deceleration parameter within their respective 1σ confidence level.

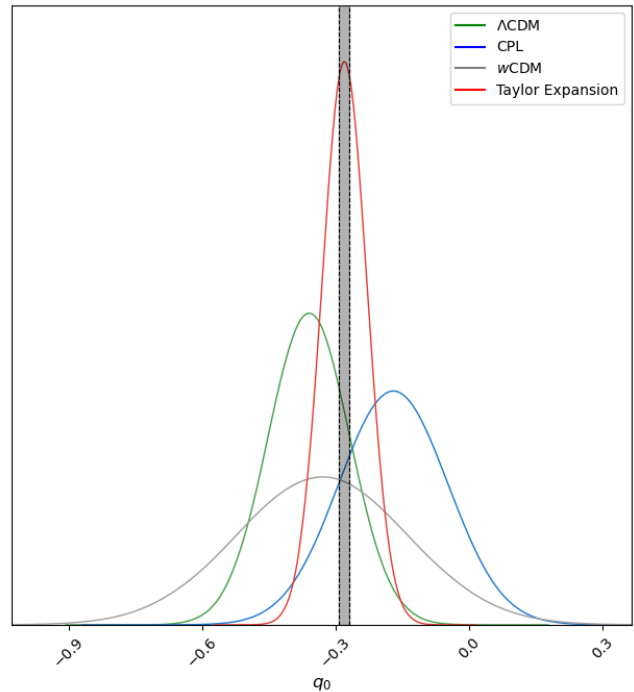


Figure 11. The probability density function of deceleration's present value for the different models studied. The shaded area shows the deceleration parameter range in agreement within 1σ confidence range of all models.

In the Pantheon+ analysis, the team combined many other researches to add more constrains on their density parameters. They combined the Pantheon+ data with the SH0ES analysis, the Planck results and Baryon Acoustic Oscillation (BAO) measurements in galaxies. These combinations gave various results for the parameters but the biggest difference they created was leading to vastly different Hubble constants; that was around 67 when combined with Planck and/or BAO, while being around 73.5 when combined with SH0ES. Such interdisciplinary analysis could highly benefit the CPL model, with a smaller Hubble constant leading to an older universe age. In addition, getting more accurate density parameters could show a more clear picture of the bizarre behavior seen in figure 7.

One possible suggestion to increase the accuracy of the CPL model and look deeper into it would be to target low redshift ranges, where the tipping point happened

and where the dark energy achieved its highest value according to the CPL model results. The more objects there are, the more accurate the results in that critical range would be. Another valid possibility is to check the model with a curvature element. This is not possible with the data in hand due to the very high errors, however with many ambitious surveys to come and larger data sets to be compiled it could be possible to use this model with a curvature parameter and get accurate results.

5. CONCLUSION

When proposed by Chavellier & Polarski in 2001 (Chavellier & Polarski (2001)), the data available for scientists at the time was limited with many systematic

errors and so the varying dark energy model did not catch the eyes of the scientific world. The results were not accurate enough to argue with the more superior model, the Λ CDM, which was given the title of the standard model of cosmology. However with the most recent Pantheon+ project, the data base was standardized, refined and a very comprehensive covariance matrix was assembled that accounted for many possible systematic errors (Scolnic et al. (2022); Brout et al. (2022a)). With these recent upgrades to the SNe Ia data, the Chavellier-Polarski-Linder model now gives accurate results with small standard deviations; results that can be discussed and put side by side with the Λ CDM model. More in depth studies must be conducted to explain, understand or correct the unexpected result this model gave.

REFERENCES

- Aghanim, N., Akrami, Y., Ashdown, M., et al. 2020, *Astronomy & Astrophysics*, 641, A6, doi: [10.1051/0004-6361/201833910](https://doi.org/10.1051/0004-6361/201833910)
- Arnett, W. D. 1969, *ApJ*, 157, 1369, doi: [10.1086/150157](https://doi.org/10.1086/150157)
- Branch, D., & Tammann, G. A. 1992, *Annual Review of Astronomy and Astrophysics*, 30, 359, doi: [10.1146/annurev.aa.30.090192.002043](https://doi.org/10.1146/annurev.aa.30.090192.002043)
- Brout, D., Scolnic, D., Popovic, B., et al. 2022a, *The Astrophysical Journal*, 938, 110, doi: [10.3847/1538-4357/ac8e04](https://doi.org/10.3847/1538-4357/ac8e04)
- Brout, D., Taylor, G., Scolnic, D., et al. 2022b, *The Astrophysical Journal*, 938, 111, doi: [10.3847/1538-4357/ac8bcc](https://doi.org/10.3847/1538-4357/ac8bcc)
- Carr, A., Davis, T. M., Scolnic, D., et al. 2022, *Publications of the Astronomical Society of Australia*, 39, doi: [10.1017/pasa.2022.41](https://doi.org/10.1017/pasa.2022.41)
- Carroll, S. M. 2001, *Living Reviews in Relativity*, 4, doi: [10.12942/lrr-2001-1](https://doi.org/10.12942/lrr-2001-1)
- Chavellier, M., & Polarski, D. 2001, *International Journal of Modern Physics D*, 10, 213, doi: [10.1142/s0218271801000822](https://doi.org/10.1142/s0218271801000822)
- Colgate, S. A., & McKee, C. 1969, *ApJ*, 157, 623, doi: [10.1086/150102](https://doi.org/10.1086/150102)
- Doggett, J. B., & Branch, D. 1985, *The Astronomical Journal*, 90, 2303, doi: [10.1086/113934](https://doi.org/10.1086/113934)
- Eigenchris. 2022, *Relativity 110b: Cosmology - FLRW Metric Derivation (3 possible geometries)*, Youtube. <https://www.youtube.com/watch?v=iERBF2.TnXo>
- Guy, J., Astier, P., Baumont, S., et al. 2007, *Astronomy & Astrophysics*, 466, 11, doi: [10.1051/0004-6361:20066930](https://doi.org/10.1051/0004-6361:20066930)
- Hogg, D. W. 1999, *Distance measures in cosmology*, arXiv, doi: [10.48550/ARXIV.ASTRO-PH/9905116](https://doi.org/10.48550/ARXIV.ASTRO-PH/9905116)
- Hoyle, F., & Fowler, W. A. 1960, *ApJ*, 132, 565, doi: [10.1086/146963](https://doi.org/10.1086/146963)
- Kessler, R., & Scolnic, D. 2017, *The Astrophysical Journal*, 836, 56, doi: [10.3847/1538-4357/836/1/56](https://doi.org/10.3847/1538-4357/836/1/56)
- Kowal, C. T. 1968, *The Astronomical Journal*, 73, 1021, doi: [10.1086/110763](https://doi.org/10.1086/110763)
- Linder, E. V. 2003, *Physical Review Letters*, 90, 091301, doi: [10.1103/physrevlett.90.091301](https://doi.org/10.1103/physrevlett.90.091301)
- Naidu, R. P., Oesch, P. A., van Dokkum, P., et al. 2022, *The Astrophysical Journal Letters*, 940, L14, doi: [10.3847/2041-8213/ac9b22](https://doi.org/10.3847/2041-8213/ac9b22)
- Perlmutter, S., Gali, S., Goldhaber, G., et al. 1997, *ApJ*, 483, 565, doi: [10.1086/304265](https://doi.org/10.1086/304265)
- Perlmutter, S., Aldering, G., Goldhaber, G., et al. 1999, *The Astrophysical Journal*, 517, 565, doi: [10.1086/307221](https://doi.org/10.1086/307221)
- Peterson, E. R., Kenworthy, W. D., Scolnic, D., et al. 2022, *The Astrophysical Journal*, 938, 112, doi: [10.3847/1538-4357/ac4698](https://doi.org/10.3847/1538-4357/ac4698)
- Phillips, M. M. 1993, *The Astrophysical Journal*, 413, L105, doi: [10.1086/186970](https://doi.org/10.1086/186970)
- Popovic, B., Brout, D., Kessler, R., Scolnic, D., & Lu, L. 2021, *The Astrophysical Journal*, 913, 49, doi: [10.3847/1538-4357/abf14f](https://doi.org/10.3847/1538-4357/abf14f)
- Porter, A. C., & Filippenko, A. V. 1987, *AJ*, 93, 1372, doi: [10.1086/114420](https://doi.org/10.1086/114420)
- Riess, A. G., Filippenko, A. V., Challis, P., et al. 1998, *The Astronomical Journal*, 116, 1009, doi: [10.1086/300499](https://doi.org/10.1086/300499)
- Riess, A. G., Yuan, W., Macri, L. M., et al. 2022, *The Astrophysical Journal Letters*, 934, L7, doi: [10.3847/2041-8213/ac5c5b](https://doi.org/10.3847/2041-8213/ac5c5b)
- Schmidt, B. P., Suntzeff, N. B., Phillips, M. M., et al. 1998, *The Astrophysical Journal*, 507, 46, doi: [10.1086/306308](https://doi.org/10.1086/306308)

- Scolnic, D., Brout, D., Carr, A., et al. 2022, The Astrophysical Journal, 938, 113, doi: [10.3847/1538-4357/ac8b7a](https://doi.org/10.3847/1538-4357/ac8b7a)
- Tripp, R. 1998, A&A, 331, 815.
<https://ui.adsabs.harvard.edu/abs/1998A&A...331..815T>
- Uomoto, A., & Kirshner, R. P. 1985, A&A, 149, L7.
<https://ui.adsabs.harvard.edu/abs/1985A&A...149L...7U>
- Valentino, E. D., Mena, O., Pan, S., et al. 2021, Classical and Quantum Gravity, 38, 153001, doi: [10.1088/1361-6382/ac086d](https://doi.org/10.1088/1361-6382/ac086d)
- Visser, M. 2004, Classical and Quantum Gravity, 21, 2603, doi: [10.1088/0264-9381/21/11/006](https://doi.org/10.1088/0264-9381/21/11/006)
- Wheeler, J. C., & Harkness, R. P. 1990, Reports on Progress in Physics, 53, 1467, doi: [10.1088/0034-4885/53/12/001](https://doi.org/10.1088/0034-4885/53/12/001)
- Wheeler, J. C., & Levreault, R. 1985, ApJL, 294, L17, doi: [10.1086/184500](https://doi.org/10.1086/184500)
- Wikipedia contributors. 2023a, SN 185 — Wikipedia, The Free Encyclopedia. https://en.wikipedia.org/w/index.php?title=SN_185&oldid=1154754955
- . 2023b, SN 1054 — Wikipedia, The Free Encyclopedia. https://en.wikipedia.org/w/index.php?title=SN_1054&oldid=1146850229

APPENDIX

A. COSMOLOGICAL PROOFS

Our first assumption of the paper is counting on the universe to be a Friedmann–Lemaître–Robertson–Walker (FLRW) universe. This seem to hold so far from the cosmin microwave background (CMB) isotropy measurements by Planck [Aghanim et al. \(2020\)](#). The FLRW metric is defined as

$$ds^2 = dt^2 - a^2(t) \left[\frac{dr^2}{1 - kr^2} + r^2 d\theta^2 + r^2 \sin^2 \theta d\phi^2 \right]. \quad (\text{A1})$$

$a(t)$ is the expansion factor and it describes how the universe is expanding, while k is the curvature constant and would take values from -1 to 1 that describes whether the universe is closed, flat or open. Derivation of the FLRW metric could be found from a wonderful youtube video by Eigenchris [Eigenchris \(2022\)](#). Using the FLRW metric one can relate the luminosity of an object with its flux when it reaches an observer. The distance the light travels after leaving the source positioned r_1 as a function of time is

$$d_R(t) = a(t) \int_0^{r_1} \frac{dr}{\sqrt{1 - kr^2}} \quad (\text{A2})$$

with the origin point always being where the light reaches the furthest. The area of the effect sphere after a source emits light would also changes with time as

$$S(t) = a^2(t) r_1^2 \int_{\text{sphere}} \sin \theta d\theta d\phi = 4\pi a^2(t) r^2 \quad (\text{A3})$$

The emitted and observed luminosity of a source with an emitted frequency of ν_1 and a period of T_1 should be

$$L_1 \propto \frac{\nu_1}{T_1} \quad (\text{A4})$$

$$L_0 \propto \frac{\nu_0}{T_0} \quad (\text{A5})$$

having a 0 to indicate the values when the signal was received. Since light follows a null geodesic ($ds^2 = 0$), the time it would take for a light signal from a source at r_1 to reach us, the receiver at $r = 0$, would be given by

$$\int_{t_1}^{t_0} \frac{dt}{a(t)} = \int_0^{r_1} \frac{dr}{\sqrt{1 - kr^2}}, \quad (\text{A6})$$

with t_1 indicating the time of emission and t_0 indicating the time of receipt. Note that the RHS only depends on the position of the source, therefore we can safely say that the this equation must hold for one period later thus giving

$$\int_{t_1}^{t_0} \frac{dt}{a(t)} = \int_{t_1+T_1}^{t_0+T_0} \frac{dt}{a(t)} = \int_{t_1+T_1}^{t_1} + \int_{t_1}^{t_0} + \int_{t_0}^{t_0+T_0}. \quad (\text{A7})$$

During one period the universe won't expand that much, so we can assume that $a(t)$ is constant to solve the integrals. This would give us

$$\frac{a_0}{a_1} = \frac{T_0}{T_1} = \frac{\lambda_0}{\lambda_1} = \frac{\nu_1}{\nu_0} = (1 + z), \quad (\text{A8})$$

which we can place in equations (A4) and (A5) to yield

$$L_0 = \frac{L_1}{(1 + z)^2}. \quad (\text{A9})$$

Since equation (2) gives $L_1 = 4\pi F_0 d_L^2$ and since Flux is luminosity per surface area, we can write

$$F_0 = \frac{L_0}{4\pi a_0^2 r_1^2} = \frac{L_1}{4\pi a_0^2 r_1^2 (1+z)^2} = \frac{L_1}{4\pi d_L^2} \quad (\text{A10})$$

to finally derive

$$d_L = a_0 r_1 (1+z). \quad (\text{A11})$$

The task here is to find how far away r_1 is, which is easy using the FLRW metric. Since we are following a light source to determine the luminosity distance we can use the fact that light follows a null geodesic, thus $ds^2 = 0$. Also taking $d\phi = 0$ and $\theta = \pi/2$ would leave us with

$$c \int_{t_1}^{t_0} \frac{dt}{a(t)} = \pm \int_{r_1}^0 \frac{dr}{\sqrt{1 - kr^2}}. \quad (\text{A12})$$

Since $H = (da/dt)/a$, we could pull dt to get

$$dt = \frac{da}{aH}$$

also since $a = 1/(1+z)$ we can easily get $da = -a^2 dz$. Putting all that in equation (A12) and renaming r_1 as r gives

$$c \int_0^z \frac{dz}{H(z)} = \int_0^r \frac{dr'}{\sqrt{1 - k(r')^2}}. \quad (\text{A13})$$

According to each k interval, the distance will take different forms,

$$r = \begin{cases} \frac{1}{\sqrt{k}} \sinh \left(c\sqrt{k} \int_0^z \frac{dz}{H(z)} \right) & \text{for open universe } k < 0 \\ c \int_0^z \frac{dz}{H(z)} & \text{for flat universe } k = 0 \\ \frac{1}{\sqrt{k}} \sin \left(c\sqrt{k} \int_0^z \frac{dz}{H(z)} \right) & \text{for closed universe } k > 0 \end{cases}. \quad (\text{A14})$$

which in return gives us equation (3). There are two ways of solving this integral: Using the Einstein equations or expanding a Taylor series.

A.1. Solution from Taylor Expansion

Check Visser (2004) for an extensive view and a proof of this solution which would give equation (6).

A.2. Solution from Einstein Equations

The Einstein equations are

$$G_{\mu\nu} = R_{\mu\nu} - \frac{1}{2}Rg_{\mu\nu} = \frac{8\pi G}{c^4}T_{\mu\nu}. \quad (\text{A15})$$

A wonderful equation that shows the relation between geometry (LHS) and physics (RHS). $G_{\mu\nu}$ is the Einstein tensor which depends on the geometry described by the metric $g_{\mu\nu}$, the Ricci tensor $R_{\mu\nu}$ and the Ricci scalar R . On the RHS we have the physics; which is described by the energy-momentum tensor $T_{\mu\nu}$, with G being the gravitational constant proposed by Newton. We will use what's called the Planck units, which counts $c = 1$. Many sources also add the cosmological constant Λ into the equation however the most recent understanding of this constant is that it is part of the universe's energy-momentum components. Therefore it is incorporated into the energy-momentum tensor. Solving the Einstein equations for the FLRW metric and an energy-momentum tensor described by a perfect fluid (with pressure p and density ρ) yields the Friedmann equations which are

$$\frac{\ddot{a}}{a} = -\frac{4\pi G}{3} \left(\sum_i \rho_i + 3 \sum_i p_i \right) \quad (\text{A16})$$

$$\left(\frac{\dot{a}}{a} \right)^2 = \frac{8\pi G}{3} \sum_i \rho_i - \frac{k}{a^2}, \quad (\text{A17})$$

where the i index refers to the different components of the universe such as matter, dark energy and so on. It is often useful to use the curvature term and turn it into a mathematical component that could be part of the summation as well, however one must keep in mind that this is not a real physical energy component. Therefore equation (A17) turns into

$$\left(\frac{\dot{a}}{a}\right)^2 = \frac{8\pi G}{3} \sum_{i(k)} \rho_i, \quad (\text{A18})$$

with $i(k)$ indicating that the curvature component is also included in the sum. We can figure out how the densities change with the scale factor easily. For a curved universe made of matter and dark energy, we can easily figure that matter density would scale with $\rho_{m,0}a^{-3}$ with the 0 index indicating the value today (this comes from $m = \rho V$). The curvature component has to be

$$\rho_k = -\frac{3k}{8\pi G a^2} \equiv \rho_{k,0}a^{-2}$$

in order to be part of the summation in equation (A17), so we can see that it scales with a^{-2} . For the evolution of the dark energy component we will have to follow some steps before reaching a conclusion, starting with the first law of thermodynamics for energy E and volume V one can write

$$dE = -p_i dV \quad (\text{A19})$$

for each i component. The volume scales with a^3 whereas the energy scales with $\rho_i a^3$ (think of it as $E = mc^2$ where $m = \rho V$). We can now write

$$d(\rho_i a^3) = -p_i d(a^3). \quad (\text{A20})$$

Using the chain rule and substituting in $p_i = w_i \rho_i$ we get

$$\frac{d\rho_i}{\rho_i} = -3(1 + w_i)a^{-1} da. \quad (\text{A21})$$

We integrate both sides to finally derive the evolution equation for any i component

$$\rho_i = \rho_{i,0} \exp\left(-3 \int_1^a (1 + w_i)(a')^{-1} da'\right). \quad (\text{A22})$$

We can see from equation (A22) that for matter $w_m = 0$ since $\rho_m = \rho_{m,0}a^{-3}$, however for dark energy we don't know what w is and therefore many different models are proposed as shown in this paper.

Going back to equation A18 and substituting in the individual components would leave us with

$$\left(\frac{\dot{a}}{a}\right)^2 = H^2 = \frac{8\pi G}{3} \left(\rho_{m,0}(1+z)^3 + \rho_{k,0}(1+z)^2 + \rho_{de,0} \exp\left(3 \int_0^z \frac{1+w(z')}{1+z'} dz'\right) \right). \quad (\text{A23})$$

I have wrote it in terms of redshift using equation (A8) with units such that $a_0 = 1$. The critical energy, which is the energy required for a flat universe, is

$$\rho_c = \frac{3H^2}{8\pi G}.$$

By substituting in $\rho_{i,0} = \Omega_{i,0}\rho_{c,0} = 3\Omega_{i,0}H_0^2/(8\pi G)$ we derive

$$H(z) = H_0 \sqrt{\Omega_{m,0}(1+z)^3 + \Omega_{k,0}(1+z)^2 + \Omega_{de,0} \exp\left(3 \int_0^z \frac{1+w(z')}{1+z'} dz'\right)} \equiv H_0 E(z). \quad (\text{A24})$$

Using equation (A24) in equation (3) would allow us to numerically integrate and find the luminosity distances as a function of redshifts via the Einstein equations. We could go even further by deriving the deceleration parameter. For that we will use equation (A16) and divide both sides with H^2 to get

$$-\frac{1}{H^2} \frac{\ddot{a}}{a} = q = \frac{4\pi G}{3H^2} \left(\sum_i \rho_i + 3 \sum_i w_i \rho_i \right) = \frac{1}{2} \left(\sum_i \Omega_i (1 + 3w_i) \right). \quad (\text{A25})$$

The value of q_0 would then be

$$q_0 = \frac{1}{2} \left(\sum_i \Omega_{i,0} (1 + 3w_i(0)) \right). \quad (\text{A26})$$

A.3. Lookback Time

Lookback time is the time that light takes to reach us. It basically describes how long into the past we are looking when we look at a source. We know that

$$\frac{da}{dt} \frac{1}{a} = H$$

and therefore if we leave dt alone we would get

$$\int_t^0 dt = t_L = \int_a^1 \frac{da}{aH}, \quad (\text{A27})$$

where we integrated from a time of t in the past to today. Using the relation of expansion factor and redshift we can rewrite equation (A27) as

$$t_L = \frac{1}{H_0} \int_0^z \frac{dz'}{E(z')(1+z')}, \quad (\text{A28})$$

which is equation (5). We could also figure out the age of the universe by integrating from the today back to the big bang, in other words from $z = 0$ to $z = \infty$.